Foaming Of polystyrene / thermoplastic starch blends
Mihai, Mihaela; Huneault, Michel A.; Favis, Basil D.

National Research Council Canada   Conseil national de recherches Canada

Canada

Journal of Cellular Plastics

http://cel.sagepub.com/

Foaming of Polystyrene/ Thermoplastic Starch Blends
Mihaela Mihai, Michel A. Huneault and Basil D. Favis
Journal of Cellular Plastics 2007 43: 215
DOI: 10.1177/0021955X07076532

The online version of this article can be found at:
http://cel.sagepub.com/content/43/3/215

Additional services and information for *Journal of Cellular Plastics* can be found at:

Email Alerts: http://cel.sagepub.com/cgi/alerts

Subscriptions: http://cel.sagepub.com/subscriptions

Reprints: http://www.sagepub.com/journalsReprints.nav

Permissions: http://www.sagepub.com/journalsPermissions.nav

Citations: http://cel.sagepub.com/content/43/3/215.refs.html

Foaming of Polystyrene/ Thermoplastic Starch Blends

MIHAELA MIHAI,[1] MICHEL A. HUNEAULT[2,*] AND BASIL D. FAVIS[1]

[1]*CREPEC, Department of Chemical Engineering, École Polytechnique de Montréal, P.O. Box 6079, Station Centre-Ville, Montréal Québec, Canada, H3C 3A7*

[2]*Industrial Materials Institute, National Research Council, 75 de Mortagne Boucherville, Québec, Canada, J4B 6Y4*

ABSTRACT: This study investigates the fabrication of extruded foams from polystyrene/thermoplastic starch (PS/TPS) blends. A specially designed twin-screw extrusion process is used for starch gelatinization, PS incorporation, polymer mixing, and blowing agent incorporation. In-line rheometry is used to monitor the viscosity of the TPS/PS blends and to evaluate the plasticizing effect of 1,1,1,2 tetrafluoroethane (HFC-134a) used as blowing agent. Differential scanning calorimetry, scanning electron microscopy, density measurement, and picnometry are used to evaluate the thermal properties, the blend morphology, and the foam cell structure. Glycerol content in the TPS phase and the TPS content in the overall blend have a strong effect on the blend viscosity and, in turn, on the ability to foam the material. The foams blown with the hydro-fluorocarbone alone have large open-cell content and their density cannot be reduced below $170 \, kg/m^3$. The addition of a small amount of ethanol however results in three-fold reductions in density and much better foam cell homogeneity.

KEY WORDS: thermoplastic starch, polystyrene, foam extrusion.

INTRODUCTION

With the increasing cost of synthetic polymers and environmental concerns over their disposal, there has been growing interest in the use of polymers derived from annually renewable sources. Starch is one of the most abundant natural polymers and it presents many

interesting characteristics. It is biodegradable, has a relatively low cost, and is a renewable resource. From a chemical point of view, starch consists of two types of macromolecules, amylose and amylopectine, which are structurally different. Both consist of polymers of α-D-glucose units and the composition ratio between the two components depends on the natural source. Amylose, a linear polysaccharide with a molar mass in the range 10^5–10^6 g/mol, is the minor component of natural starch. Amylopectine is a branched polysaccharide with a larger degree of polymerization and a molecular mass about 10^8 g/mol.

Dry starch is tightly packed into dehydrated granules with origin-specific shape and size (2–10 μm in diameter). The crystalline starch structure disappears when it is subjected to temperatures greater than 70–90°C in the presence of a plasticizer, such as water. This transformation is called gelatinization. Because of its high molecular weight, relatively high plasticization levels are necessary for gelatinized starch to flow. Gelatinization along with some molecular weight reduction can be achieved using extrusion technology, which provide, in a closed pressurized environment, sufficient heat and shear stress to break down the crystalline structure of the semi-crystalline starch and render it completely amorphous. Once the starch is properly plasticized, it can flow just as any synthetic polymer and is therefore suited for conventional molding and extrusion technologies. This plasticized and destructured starch is referred to as thermoplastic starch or TPS.

Because of its polar nature and low molecular weight, water is probably the most efficient plasticizer for starch but it leads to material properties that are highly dependent on the humidity level. This is not suitable in most material applications. Thus, less volatile plasticizers for starch must be used. The plasticizer must be polar to ensure its compatibility with starch macromolecules. Its molecular weight must be low enough to easily penetrate the starch macromolecular network, but at the same time, its boiling point must be high enough to guarantee that it will not migrate or evaporate out of the material. Glycerol has been the most widely studied plasticizer for starch due to its high boiling point, availability, and low cost [1–7]. It was shown several years ago that extrusion at 150°C in a twin-screw extruder in the presence of a mixture of water and glycerol as plasticizers resulted in complete starch gelatinization. The gelatinization was assessed by looking at the extrudates under polarized light to detect non-gelatinized particles by their birefringence and by calorimetry [1]. The mechanical energy transferred to the blend, monitored through the measurement of extruder screw torque was shown to decrease with the total plasticizer content as expected by the plasticizing effect on melt viscosity.

The extrusion operation has a direct effect on the starch crystallinity but it was also shown that by performing the gelatinization in the presence of water and glycerol, the amylopectine molecular weight could be reduced by two orders of magnitude [2]. When using low total (water and glycerol) plasticizer content, glycerol was shown to better protect the starch from degradation probably because it lubricated the flow and decreased the stresses in the extruder. Another consequence of the starch destructuring is the modification of the amylose/amylopectine ratio. Since the branched amylopectine is most affected by the mechanical energy, its content decreases, resulting in a higher content in linear polysaccharide [4]. In turn, this leads to a decrease of the melt viscosity and to a higher flexibility for the final material. In terms of processing, the twin-screw extruder was shown to be more suitable for starch gelatinization and plasticization due to its higher mixing intensity as compared with the single screw extruder [8,9].

The rheology of TPS has been studied extensively [3,7,10–15]. By definition, a plasticizer should increase the chain mobility and lower the glass transition temperature. TPS was shown to be shear thinning and to follow a power-law behavior in the normal processing shear-rate range. An analytical description of plasticizer and temperature effect on the viscosity of plasticized starch has been proposed based on experimental observations [15]. The plasticized starch viscosity–temperature relationship was shown to obey an Arrhenius type relation in which the activation energy, instead of being constant, was a function of the plasticizer content.

The typical drawbacks of TPS are its moisture sensitivity and low temperature resistance. The mechanical properties of the water-glycerol plasticized starch were also shown to vary during time following the sample fabrication. Loss of glycerol and recrystallization can lead to a three-fold increase in tensile modulus and dramatic reduction in elongation at break after 5 weeks of aging [2]. To prevent these changes and to fine tune the properties, there has been a considerable effort devoted to blends of TPS with other biodegradable and non-biodegradable polymers. In all cases, the addition of the second polymer phase mainly aims at controlling the plasticized starch hygroscopy, at reducing the plasticizer migration, and at tuning the materials properties toward the specific applications.

Plasticized starch has been blended with both biodegradable and non-biodegradable polymers. In the former category, biodegradable blends were reported with biodegradable polyesters, such as polyesteramide [16,22], poly (lactic acid) [17,18,22], poly (ε-caprolactone) [19–21],

poly (butylene adipate terephthalate), and poly (butylene succinate adipate) [22]. As for non-biodegradable polymers, it has been shown that TPS can be incorporated into polyethylene while maintaining the high elongation properties at break even at plasticized starch contents up to 40% [5–7].

Materials based on TPS have only recently become commercially available at an industrial scale and are still relatively expensive because they typically include a specialty polymer, such as ethylene-vinyl alcohol copolymer, aliphatic biodegradable polyesters, or cellulose derivatives. One important utilization of TPS is in the form of cushioning and protective packaging known as loose filler. Because of their low density, the disposal of loose fillers is an important concern. The TPS loose filler has the advantage that it can be dissolved in water to reduce its volume and can be composted. In this case, the water-solubility of the TPS is seen as an advantage over the non-biodegradable non-soluble polystyrene (PS) [23]. The starch-based foams also show antistatic properties as compared to expanded PS foams [24].

For water-soluble foam applications, the addition to starch of several biodegradable polymers including poly(lactic acid), poly(hydroxyester ether), poly(hydroxybutyrate-co-valerate), poly(butylene-succinate), poly(caprolactone), poly(vinyl alcohol), and poly(ester amide) has been thoroughly investigated [25]. The density of water-foamed starch controls reached $60\,kg/m^3$. Addition of the biopolyesters in the 10–20% range helps to further decrease the foam densities in the $20–60\,kg/m^3$ range while maintaining high water absorbsion. Non water-soluble foams from starch/PS and starch/PMMA blends were also investigated [26]. In this case, chemical blowing agents (sodium bicarbonate and urea) were used in combination with a cross-linking agent. Foam densities in the range of $30–130\,kg/m^3$ were obtained, with radial expansion ratios of 8.8–40.

The purpose of this work is to evaluate the morphological and physical properties of foamed TPS/PS blends for partial substitution of PS in non-biodegradable, non-water soluble commodity packaging or insulation applications. In contrast to water-foamed starches, the current work will focus on achieving water-free materials that may be more suitable for longer-term applications. The foaming of plasticized starch/PS will be carried using a hydrofluorocarbon, HFC-134a, which is a zero ozone-depleting-potential (ODP) blowing agent. The partial substitution of the PS by plasticized starch could be a step toward an increased use of renewable resources without sacrificing useful PS foam properties.

<div align="center">

EXPERIMENTAL DETAILS

</div>

Materials

The PS grade was AtoFina 523 resin. It has a melt index of 11 g/ 10 min, a weight average molecular weight $Mw = 208{,}000$, and a polydispersity Mw/Mn of 2.63. The starch was Supergell 1203-C wheat starch from ADM-Ogilvie composed of 25% amylose and 75% amylopectin. Distilled water and glycerol (99.5 vol%) obtained from SIMCO Chemical Products Inc. were used for gelatinization and plasticization of starch. The blowing agent was 1,1,1,2 tetrafluoroethane also known as HFC-134a supplied by AtoFina. Talc powder was used at 0.5 wt% as a nucleation agent in all foams.

The starch was fed in the form of a suspension in a glycerol-water mixture. As will be discussed in detail below, the water is removed during the process through devolatilization. The TPS can therefore be specified in terms of its glycerol content. All suspensions contained initially 25 wt% of water and the glycerol and starch concentration were adjusted to obtain five different glycerol contents in the water-free material. A 7% humidity content in the native starch was accounted for in the final glycerol content calculation, assuming that all the water is vented out from the TPS polymer. The plasticized starch presented in this study will be referred to as TPS30, TPS34, TPS39, TPS42, and TPS47 for starch plasticized with 30, 34, 39, 42, and 47 wt% of glycerol, respectively.

Processing

The procedure used to prepare the blends was based on earlier work reported by Rodriguez-Gonzalez et al. [6] to produce a glycerol plasticized starch in blend with PE. In the current study, the twin-screw extrusion process was adapted to incorporate and dissolve the blowing agent into the polymer in the second half of the extruder. A sketch of the screw configuration and operation sequences is presented in Figure 1. The extruder is a Leistritz 34 mm co-rotating twin-screw extruder. It was operated at a screw rotation speed of 150 rpm and for total flow rates ranging from 5 to 10 kg/h. A suspension made from starch/glycerol/water was fed in extruder segment 0 (see Figure 1 for segment numbering) using a volumetric pump. Precise feed rate values were measured by monitoring the loss-in-weight on the starch suspension reservoir.

The first two extruder segments after feeding are used to heat and gelatinize the starch. The temperatures in segments 1–2 were
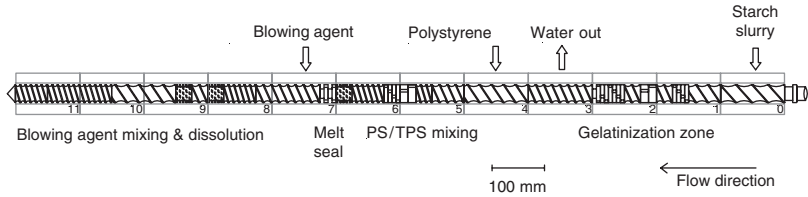
Figure 1. Schematic of screw configuration and sequence of operations.

70 and 90°C. Section 3, operated at 110°C is used to remove the water under vacuum to obtain a water-free glycerol plasticized TPS. Molten PS was pumped into the twin-screw Segment 4 using a 25 mm single-screw extruder. The feed rate of the PS was also monitored using a loss-in-weight feeder. The PS and TPS were mixed together in Segments 5–6 operated at 180°C. The blowing agent was pumped in barrel Segment 7 using a HPLC pump and the rest of the extruder length was used to solubilize the blowing agent in the polymer blend and to bring the material temperature to the desired final extrusion temperature. The screw configuration was designed to conceal the high blowing agent pressure used in the latter portion of the extruder. This was achieved by placing two pairs of shear disks upstream from the blowing agent injection point. These screw elements generate a restriction to polymer flow, increase the pressure locally, and thus create a polymer melt seal that prevents leakage of the blowing agent upstream. A gear pump was placed at the end of the extrusion line. The gear pump was used to maintain a high-pressure level in the extruder and to prevent premature bubble nucleation prior to the polymer exit from the extrusion die.

For all unfoamed blends, the extrusion temperature in the second half of the extruder was maintained at 180°C. For the foamed blends, the temperature was adapted as a function of the blowing agent concentration. In the foaming process, the solubilization of the blowing agent leads to plasticization, and thus to a drop in the polymer blend viscosity. To maintain sufficient melt strength during foaming, it is a common practice to reduce the material temperature as the concentration of blowing agent is increased. This approach was adopted here and consequently the foam extrusion temperature was reduced from 180°C progressively down to around 120°C for the blends containing the maximum blowing agent content of 7%. In all cases, the materials were extruded through a cylindrical die having a diameter of 2 mm.

On-line Rheological Characterization

The viscosity was measured at the end of the twin-screw extruder with a commercial on-line rheometer, Process Control Rheometer PCR-620 from Rheometric Scientific. The instrument is mounted in such a manner that a stream of the melt is drawn continuously from the process and brought to a rectangular slit die. The pressure gradient is measured with two pressure transducers while the volumetric flow rate is controlled through metering pumps. This allowed the determination of the melt viscosity over a range of shear rates. The unfoamed blend viscosity was measured for imposed shear rates between 0.5 and $20\,s^{-1}$ at 180°C. For the blends containing blowing agent, the shear rate was varied from 1 to $170\,s^{-1}$ at 150°C. One key advantage of on-line rheometry is that it enables measurement at a controlled hydrodynamic pressure. In this work, the viscosity measurements were made under a pressure of 5 MPa. Maintaining a sufficient pressure level is essential to prevent gas–liquid phase separation (i.e., foaming) of the polymer/blowing agent mixtures in the rheometer. In all cases, Rabinowitsch corrections were applied to take into account the effect of shear-thinning on the true shear rate determination. The final portion of the extruder and the rheometer were always operated at the same temperature.

Differential Scanning Calorimetric Analysis (DSC)

Differential scanning calorimetric analysis was carried out by means of a heat-cool-heat method. The pure TPS and the TPS/PS blends samples were sealed in aluminum pans (10 mg). The second heating cycle was used to estimate the glass transition temperature of TPS materials. The temperature was varied from −100 to 200°C, 10°C/min.

Scanning Electron Microscopy (SEM)

Prior to the SEM observation, the unfoamed blends were cryogenically fractured in liquid nitrogen and the TPS fraction was extracted from the blends in a stirred solution of HCl 6N at 60°C for 96 h. Extracted samples were vigorously washed with distilled water and dried in a vacuum oven for 72 h. The foamed samples were fractured perpendicular to the extrusion direction. They were fractured at room temperature when they comprised less than 50%TPS. The ones with greater than 50%TPS, which are softer, were fractured in liquid nitrogen. All surfaces were sputtered with a gold/palladium alloy.

Blowing Agent Pressure

The gas injection pressure was recorded, not only because this is of practical importance from a technological point of view, but also because it gives a direct indication on the solubility of the blowing agent. This was achieved by measuring the gas pressure at the gas injection point in the second part of the extrusion line. This extruder portion is only partially filled by the polymer. Since the polymer is simply conveyed in that portion, it exerts very little pressure. Therefore, the measured pressure corresponds essentially to the gas pressure exerted by the blowing agent on the polymer-blowing agent solution. The pressure-concentration data generated by this method is similar to solubility data obtained in a closed vessel using a microbalance but characterizes the material in dynamic conditions.

Foam Characterization

The density of the foams was determined by a water immersion method. In these measurements, at least three specimens were considered for each formulation. Open-cells percentage for the foams was determined with Piccnometer AccuPyc 1330. The used method corrects for the cut cells using two separate measurements. For the second measurement, the sample was cut to double the cut surface and the difference in open-cell volume was applied as a correction to the initial measured volume.

RESULTS AND DISCUSSION

Rheology

Figure 2 presents the shear viscosity of PS and TPS at $180°C$ as a function of shear rate. Measurements were made using on-line rheometry described earlier. This ensures measurement conditions that are much more representative of processing conditions than off-line measurement where the TPS water and plasticizer content may change during the test. All materials exhibit a shear-thinning power-law behavior with PS being the most viscous material. The viscosity of the TPS decreases with the glycerol plasticizer content thus increasing the viscosity ratio between the PS and TPS phase. If one compares the materials at a shear rate of $10\,s^{-1}$, the PS viscosity is 1.75 times greater than the viscosity of TPS30, containing 30% glycerol. This ratio increases to a value of 14 for the TPS47 comprising 47% glycerol.
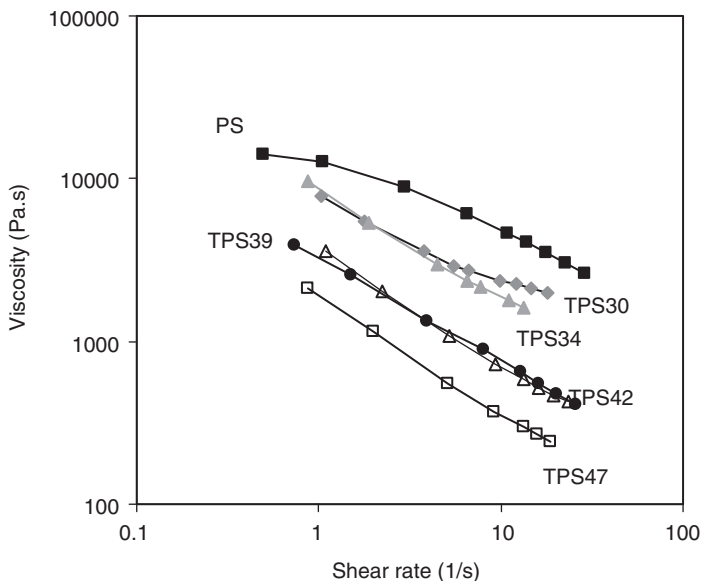
Figure 2. Viscosity as a function of shear rate for TPS and PS at 180°C.

Viscosity dependence over the glycerol content could be attributed to a dilution effect as well as to a depression in the glass transition temperature, T_g, of the blend. The decrease in the T_g was measured directly by differential scanning calorimetry and is shown in Figure 3. The T_g of the TPS30 is $-57°C$ and decreases progressively to $-70°C$ as the glycerol content is increased up to 47%. This is a sign of plasticization but calculations using the WLF model clearly show that the T_g shift is insufficient to explain the large viscosity depression and therefore, part of the viscosity reduction can be attributed to a dilution effect, or in simple terms to the substitution of the high viscosity polysaccharide by the lower viscosity glycerol. The measured T_g values for water-free TPS are in the same range as those found by Rodriguez-Gonzales et al. [7] and Forssell et al. [2].

The viscosity of the PS/TPS blends was measured over the complete blend composition range and are compared in Figure 4 for a shear rate of $10 \, s^{-1}$. The blend viscosity is always slightly lower than that expected from a log-linear mixing rule. In fact, the viscosity of blends comprising 30% and more of TPS are fairly similar to that of the pure TPS. This is especially true for the high glycerol content TPS for which the viscosity differences with the PS are greater. This could be explained by excess
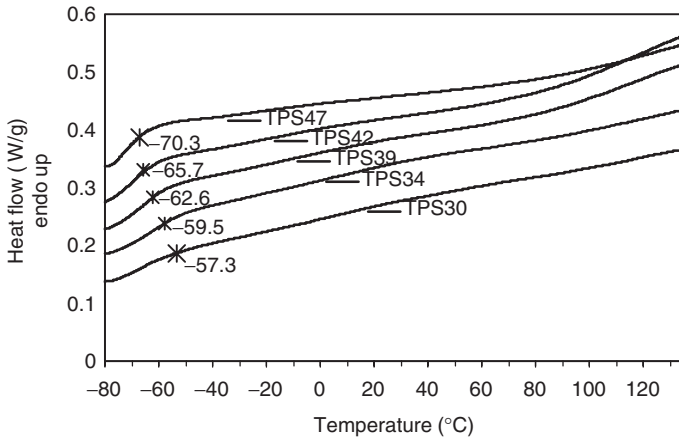
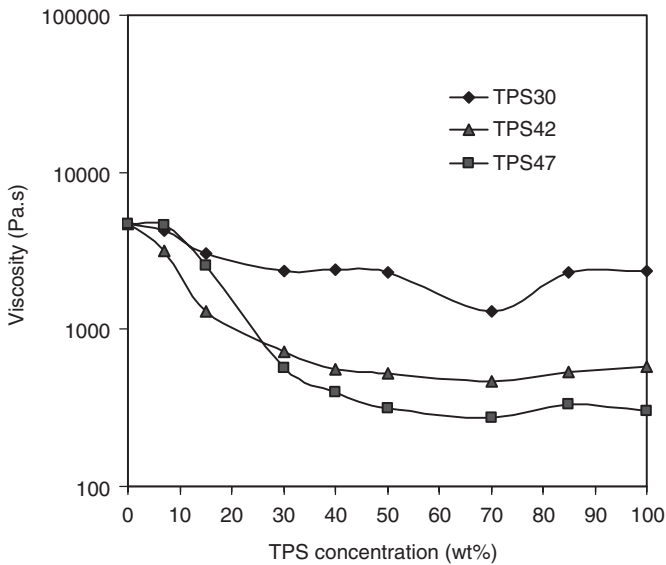**Figure 3.** Heat flow curve for TPS as determined by DSC analysis.

Figure 4. Viscosity at 180°C as a function of TPS concentration at a constant shear rate of $10\,s^{-1}$.

glycerol that phase separates and lubricates the flow leading to a low viscosity that is independent of composition.

Figure 5 presents the effect of the blowing agent concentration on the viscosity of TPS30, TPS34, and PS. As expected, the viscosity drops with the blowing agent content due to its plasticization effect. As for glycerol,
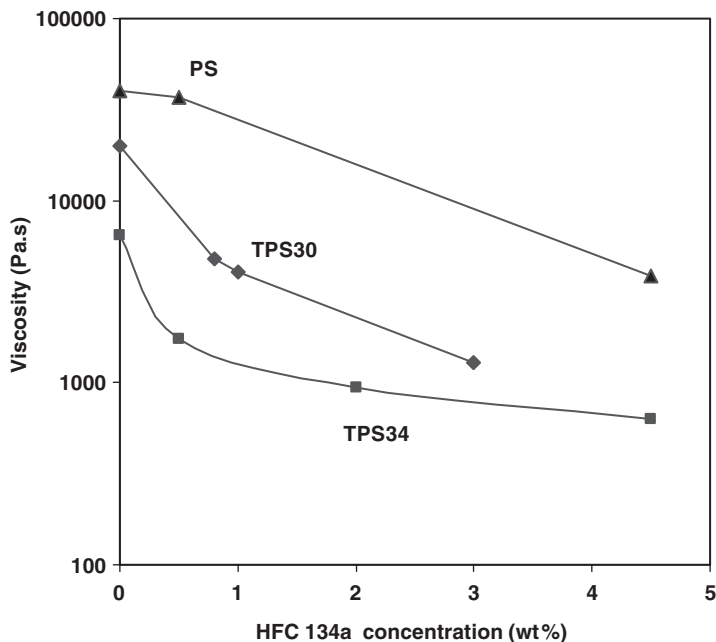
Figure 5. Viscosity as a function of HFC-134a concentration for TPS and PS at $150°C$ for a shear rate of $10 \, s^{-1}$.

the blowing agent reduces the materials glass transition further reducing its viscosity. In the case of the TPS, the viscosity drops more rapidly at the low blowing agent concentration. This may be indicative that the solubility limit has been reached and that further viscosity reduction is due to a dilution effect rather than by a classic plasticization effect. Similar results were found with different blend compositions for TPS30/PS and TPS34/PS. For the higher glycerol content, 39 and 47%, the viscosity dropped to less than 10 Pa.s, a range that was below the measurement range of the on-line rheometer.

Blend Morphology

The TPS and PS form an immiscible blend in which the morphology depends on the viscosity ratio between the TPS and the PS phase, on the blends interfacial properties, and on the process history related to the extruder configuration and operating conditions. Figure 6 presents scanning electron micrographs (SEMs) for the TPS30/PS and the TPS47/PS blend series. It is noteworthy for the morphological analysis
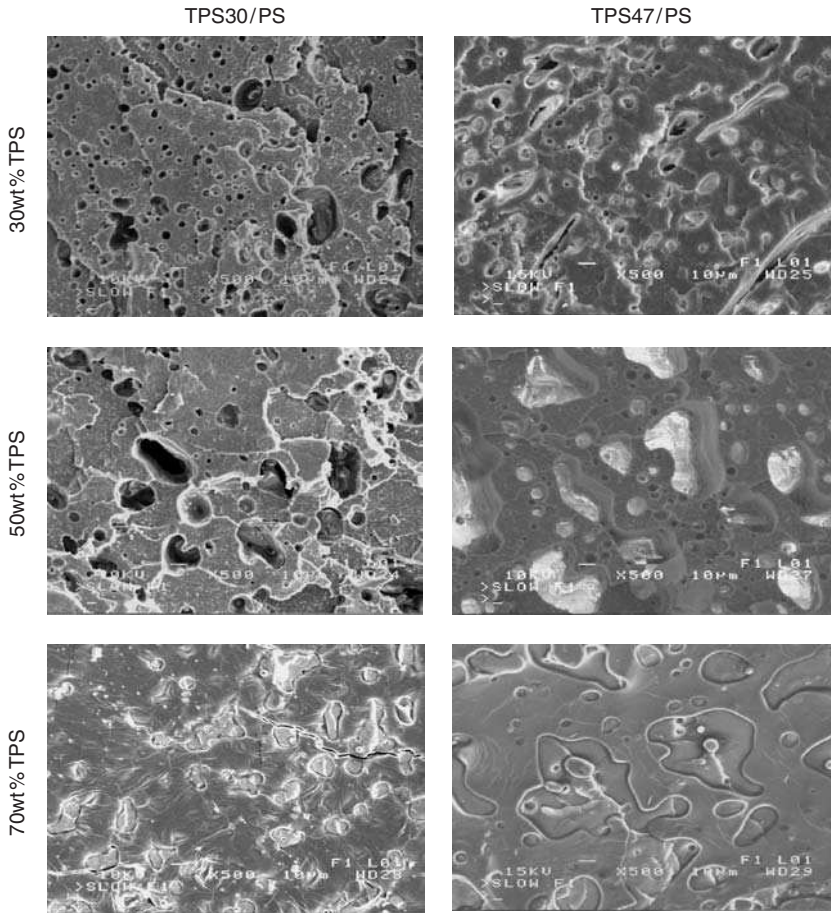
TPS30/PS   TPS47/PS

Figure 6. SEM morphologies for TPS30/PS and TPS47/PS blend series at 30, 50, and 70 wt%TPS. Samples at 70 wt%TPS are without TPS extraction. The scale bars refer to 10 μm.

that because of the density difference between the TPS (around 1.35) and the PS (1.05), the TPS volume fraction is smaller than its mass fraction. The 30, 50, and 70 wt% TPS correspond respectively to 25, 44, and 64 vol%. For the first blend series (left column micrographs on Figure 6), at 30 wt% TPS, the TPS forms the dispersed phase with spherical particles in the 5–10 μm range. At 50 wt% TPS, the TPS phase forms a mixture of large domains in the 20–100 μm range and of smaller spherical particles in the 2–10 μm range. When the TPS30 concentration is pushed to 70 wt%, the phases are inverted and the PS becomes the

dispersed component with a droplet size in the 10–20 μm range. For the TPS47/PS blend series, the TPS phase is one order of magnitude less viscous than in the previous blend series. Nonetheless, at 30 wt% TPS47, the TPS phase size is not significantly different from that observed for the TPS30/PS except for the presence of a few highly elongated particles. This is an additional indication that the TPS is already well plasticized at 30 wt% glycerol [6]. Further addition of glycerol leads to partial phase separation as suggested from the rheology results and do not change the deformability of the glycerol-saturated TPS phase. Since the PS is the most viscous component in both blend series, the blend morphology in blends where the PS is the matrix should not be limited by minor phase deformability. It can therefore be expected that the morphology will not be very sensitive to TPS viscosity at low TPS concentration. The morphology obtained at 50 wt% TPS for the TPS47 is still relatively similar to that obtained with the more viscous TPS30. It is really at 70 wt%, when the TPS becomes the major component in volumetric terms that there is a significant difference between the blends. The low viscosity of the TPS47 material does not lead to sufficient stress transfer to deform and disperse the PS phase, leading to an extremely coarse morphology in which the PS domains reach up to 100–150 μm.

Blowing Agent Injection Pressure

Figure 7 presents the effect of blowing agent concentration on the gas pressure measured over the gas–polymer solution in the extruder at 150°C at the gas injection point. The blowing agent is injected in a zone that is not pressurized by the polymer flow. By definition at steady-state, the blowing agent solubilization rate must equal its feed rate in the extruder. Since the blowing agent feed rate is fixed by the operation, the only variable in the system is the blowing agent pressure, which must adjust itself to a level that provides the required solubilization rate. In that sense, the relationship between the measured gas pressure and the blowing agent feed rate is analogous to a classical pressure-solubility measurement except that it is measured in a dynamic environment and it may be slightly increased by a pressure contribution due to the polymer flow. The classical data of Sato et al. [27] obtained for PS in quiescent equilibrium conditions are presented in the same figure for reference. The measured HFC-134a gas pressure increases with its feed rate as expected and is in the 0–3 MPa range for the typical 0–5 wt% blowing agent range. These pressures are in the same order as those expected in PS from Sato's solubility data and are in an acceptable range for foam extrusion. No special process modifications are therefore
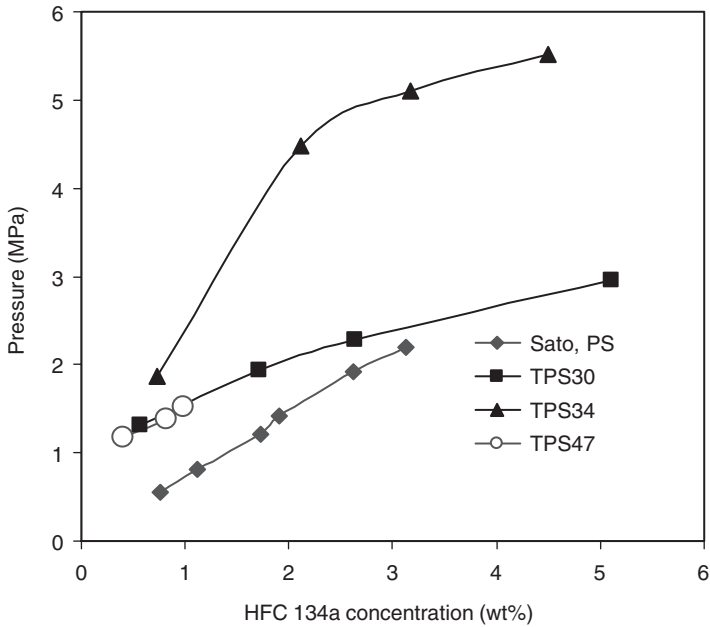
Figure 7. Comparison of HFC-134a solubility between pure TPS and PS.

required to accommodate for the presence of the TPS in the PS/TPS blends.

Foam Properties

TPS/PS blends of various compositions were foamed with 0–5 wt% blowing agent. The foam density for the blend series with TPS30, TPS34, TPS39, and TPS47 are presented in Figure 8 as function of blowing agent concentration. Overall, the lowest densities were achieved in blends with the TPS containing 30 wt% glycerol. The density obtained with pure PS is presented as a reference. The PS foam density decreases continuously for blowing agent concentrations up to 7%. A density of $60 \, kg/m^3$ was achieved for the pure PS foam controls. In the case of TPS/PS blends, the density decreases rapidly with the addition of up to 2 wt% of blowing agent but then levels off. For the TPS30/PS series, the 30% TPS and 50% TPS blends reach densities in the $200–250 \, kg/m^3$. The density of the 85% TPS30 blend reaches a minimum of $170 \, kg/m^3$ for 0.8 wt% blowing agent and then increases rapidly for higher blowing agent contents. For the blend series with the TPS containing 34%
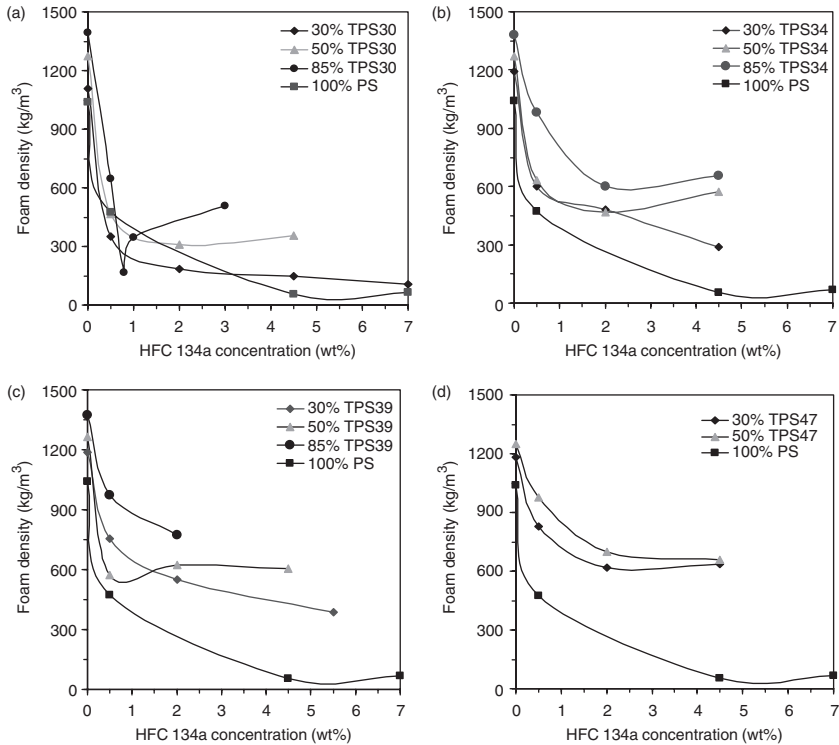
Figure 8. Variation of foam density as a function of HFC-134a concentration for: (a) TPS30/PS, (b) TPS34/PS, (c) TPS39/PS, and (d) TPS47/PS blends.

glycerol, the achieved foam densities were in the range 300–600 kg/m^3 while for 39% glycerol, the densities were in the range 400–900 kg/m^3. The blends with the TPS47 were very difficult to foam and showed evident signs of cell collapse resulting in limited density reductions.

From the density reduction data, it is clear that the blends with the most viscous TPS are better suited for foam extrusion as they have better melt strength during foaming, thus preventing the foam collapse. Even with the TPS30 however, the foam density levels off after adding 2 wt% blowing agent. One factor that can limit the effect of a blowing agent is cell rupture and therefore the closed cell content of the produced foams was investigated. The open-cell content is defined as the relative fraction of cells that are interconnected because of cell wall rupture. It was found that for all blends foamed with 2 wt% blowing agent, the open-cell content varied between 90 and 100%. Under the same conditions, the open-cell content for the PS reference is 20%. For the

85%TPS30/PS blend foamed with 0.8 wt% blowing agent, the open-cell content is also close to 100%. It appears that the TPS, even at low concentrations, is weakening the cell walls and induces cell rupture. In this context, the blowing agent is able to escape from the foam and thus loses its blowing power. Thus, the open-cell content largely explains why density is not sensitive to blowing agent concentration over a threshold value.

The foam cell structure has been investigated by scanning electron microscopy on fractured surfaces and is presented in Figures 9–11. As the lowest density foams were obtained with the TPS30/PS series, the study focuses on this blend series. Figure 9 compares the cell structures obtained for various concentrations of TPS30 foamed with only 2% HFC-134a. Figure 9(a) presents the morphology of the pure PS as a reference. It must be noted that at this low blowing agent concentration, the PS foam exhibits large and relatively non-uniform cells. The observed PS cell size ranges from 100 to 200 µm. Comparable cells dimensions are obtained with the 30%TPS blend, which exhibited a density in the 190 kg/m^3. At 50%TPS, the foam density has nearly
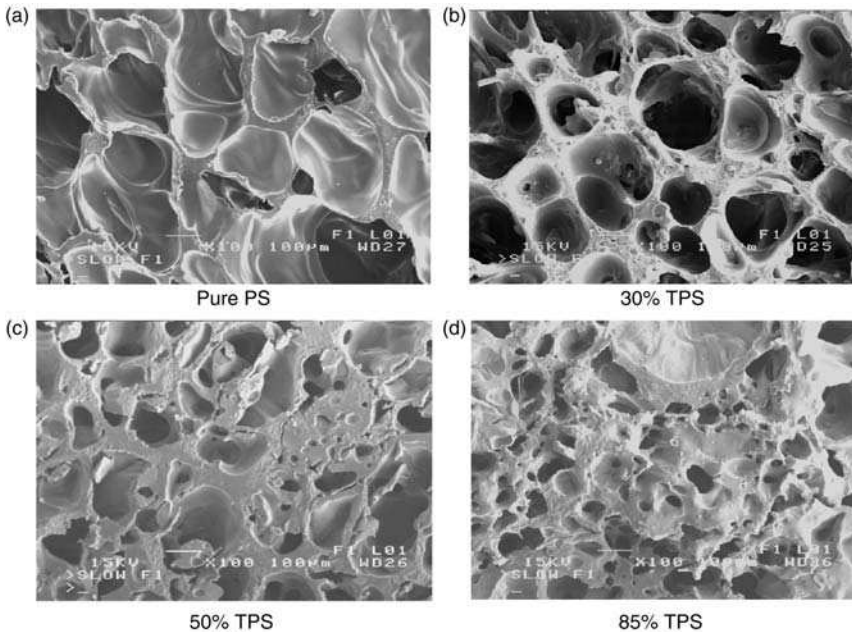

Figure 9. Morphology of PS/TPS30 blends foamed with 2% HFC-134a for (a) 0% TPS, (b) 30% TPS, (c) 50% TPS, and (d) 85% TPS. The scale bars refer to 100 µm.
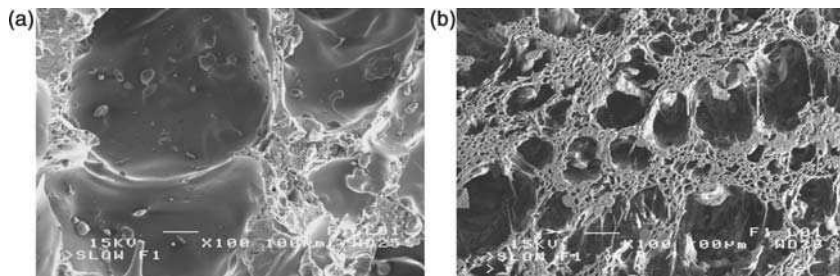
Figure 10. Morphology of 30%TPS30 blends foamed with HFC-134a concentration of (a) 0.5% and (b) 7%. The scale bars refer to 100 μm.
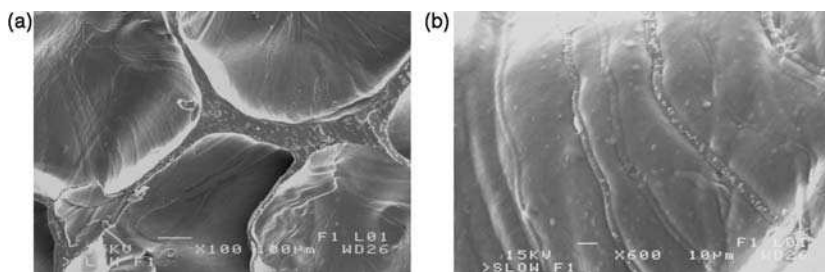

Figure 11. Foam morphology in 85% TPS30 foamed with 0.5% HFC-134a. Figure (a) shows a general view and Figure (b) shows details in the cell wall. The scale bars refer to 100 μm and 100 μm respectively.

doubled and this clearly shows up in the micrographs as seen by a thickening of the cell walls and apparent collapse of the cells. The 85%TPS30 foam, with 2% blowing agent, exhibits an even smaller cell size and completely collapsed cells.

Figure 10 presents the foam morphologies for the 30%TPS30/PS blend for the lowest and highest blowing agent concentration used in the study. These micrographs can be compared with the 2% blowing agent foam already presented in Figure 9(b). At 0.5% blowing agent, cell rupture is reduced and the observed foam morphology is reminiscent of the pure PS foam morphology. It is noteworthy that some TPS domains can be seen within the cell walls. At the other extreme, Figure 10(b) presents the foams obtained with 7 wt% blowing agent. The density of this foam is 110 kg/m^3, slightly lower than that with the 2% blowing agent one, but its morphology is strikingly different. Large cells in the 100–200 μm range are still present, but a population of smaller 5–20 μm cells has grown within the cell walls. When achieving low-density foams with high concentration of blowing agent, the cell walls are progressively
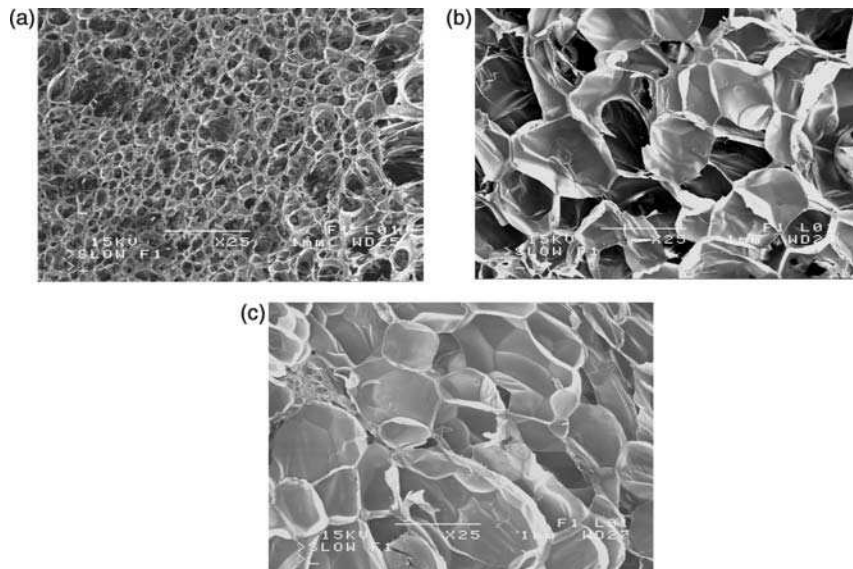
Figure 12. Scanning electron micrographs for 30%TPS30 foamed blend with 2% HFC-134a with increasing ethanol content of (a) 2%, (b) 4.5%, and (c) 6%. The scale bars refer to 1 mm.

thinned down and the blowing agent can more easily diffuse from its solution state to the gas bubble. In the current case, the cell wall thinning is stopped early in the process due to the open-cell structure, which relieves the gas pressure and prevents further cell expansion. In this situation, the excess concentration of blowing agent that is still trapped in the blend forms a second population of cells of much smaller dimension. Therefore, the remaining blowing agent forms a second foam structure within the relatively thick cell walls instead of contributing to the large cell growth as in closed-cell foams.

As noted in the density data and earlier micrographs, the presence of the TPS in the TPS/PS blends generally leads to poorer foamability and increased density. One striking exception is the 85%TPS30/PS blends foamed with only 0.8 wt% blowing agent. This foam exhibits a relatively low density ($170 \, kg/m^3$) compared to the other blends comprising lesser amounts of TPS. Further efforts on the morphology of this blend have unveiled a peculiar blend morphology presented in Figure 11. A low magnification SEM in Figure 11(a) shows large cells similar to other foams obtained at low blowing agent concentration. Surprisingly, if one focuses at higher magnification on the cell walls, one can systematically see elongated PS fibrils with a diameter of 5–7 µm. At this blend

composition, the TPS matrix seems to be reinforced by these fibrils leading to relatively low-density material. Similar features were observed in 85%TPS/PS foams, with the lower viscosity TPS34 and TPS39. In these cases, the PS fibers were thicker reaching diameters of 7–10 μm and 15–20 μm, respectively. To the authors' knowledge, it is the first time such peculiar blend morphology is reported in the literature. For polymers that do not have sufficient melt strength for foaming, this new structure could be a manner for reinforcing the cell walls.

A high open-cell content is not desired in most applications and in the current study it has been identified as a key obstacle for reducing the densities of TPS/PS foams. One potential route for decreasing open-cell content is to decrease the blowing power by incorporating less volatile components in the polymer-blowing agent solution. To validate this approach, ethanol was added to the formulations in concentration between 2 and 6%. Because of its polar nature, ethanol can be expected to be highly soluble in the TPS but was also reported to be 10 times more soluble in PS than HFC-134a [28]. The morphology for 30%TPS30/PS blends foamed with 2 wt% of the HFC-134a blowing agent in presence of ethanol is presented in Figure 12. At 2 wt% of ethanol, the cell size is in the 100–200 μm range, similar to that observed in Figure 9(b) for the blend without ethanol. At 4.5 and 6% ethanol, the cells have grown to around 1 mm and the cell walls have been thinned down dramatically. These are clear signs that bubble growth can proceed to a much greater extent. This is confirmed by the measured density of 60 kg/m^3 for 2 and 4% ethanol and of 50 kg/m^3 obtained for 6% ethanol. The use of small amounts of isopropanol, which has a relatively similar volatility and chemical nature than ethanol, has been reported to improve foam homogeneity and decrease density for neat PS foams [29]. Improvements have been explained through additional plasticization of the PS that favors bubble growth and possibly through improved diffusion of the HFC-134a into the polymer. Similar mechanism may explain the improvement observed in TPS/PS foams when adding ethanol to the HFC-134a blowing agent.

CONCLUSIONS

Foams from thermoplastic starch/polystyrene (TPS/PS) blends can be achieved in a one-step extrusion process. The glycerol content in the TPS is the most important parameter controlling the rheology and foamability of the blends. The viscosity of the TPS was shown to

decrease significantly with the glycerol concentration which was varied from 30 to 49% of the TPS phase (dry basis). The lowest density foams had a density in the 170–250 kg/m^3 range. These were achieved with the lowest glycerol content TPS and at a TPS concentration of 30 wt%. Increasing the glycerol content in the TPS or increasing the TPS concentration in the blend decreased the melt strength of the material leading to more cell collapse and to increased density. For all blends, it was also shown that density decreases rapidly when adding up to 1–2 wt% of blowing agent but then levels off at higher blowing agent content. Cell opening was shown to limit the blowing power and thus the attainable density reduction by prematurely relieving the gas pressure in the foam. This problem was circumvented however by the addition of ethanol to the mixture. The presence of ethanol was found to be very effective in obtaining a more homogeneous cell structure. Foams with densities down to 50 kg/m^3 were achieved by using a combination of HFC-134a and ethanol as blowing agents.

REFERENCES

1. Van der Burgt, M.C., Van der Woude, M.E. and Janssen, L.P.B.M. (1996). The Influence of Plasticizer on Extruded Thermoplastic Starch, *Journal of Vinyl & Additive Technology*, **2**(2): 170–174.

2. Forssell, P., Mikkilä, J. and Suortti, T. (1996). Plasticization of Barley Starch with Glycerol and Water, *J.M.S. Pure Applied Chemistry*, **A33**(5): 703–715.

3. Yu, J., Chen, S., Gao, J., Zheng, H., Zhang, J. and Lin, T. (1998). A Study on the Properties of Starch/Glycerin Blends, *Starch*, **50**(6): 246–250.

4. De Graaf, R.A., Karman, A.P. and Janssen, L.P.B.M. (2003). Material Properties and Glass Transition Temperatures of Different Thermoplastic Starches After Extrusion Processing, *Starch*, **55**: 80–86.

5. St-Pierre, N., Favis, B.D., Ramsay, B.A., Ramsay, J.A. and Verhoogt, H. (1997). Processing and Characterization of Thermoplastic Starch/Polyethylene Blends, *Polymer*, **38**(3): 647–655.

6. Rodriguez-Gonzalez, F.J., Ramsay, B.A. and Favis, B.D. (2003). High Performance LDPE/Thermoplastic Starch Blends: a Sustainable Alternative to Pure Polyethylene, *Polymer*, **44**: 1517–1526.

7. Rodriguez-Gonzalez, F.J., Ramsay, B.A. and Favis, B.D. (2004). Rheological and Thermal Properties of Thermoplastic Starch with High Glycerol Content, *Carbohydrate Polymers*, **58**: 139–147.

8. Souza, R.C.R. and Andrade, C.T. (2002). Investigation of the Gelatinization and Extrusion Processes of Corn Starch, *Advances in Polymer Technology*, **21**(1): 17–24.

9. Binduz, W., Livings, S.J. et al. (2002). Glass Transition of Extruded Wheat, Corn and Rice Starch, *Starch*, **54**: 393–400.

10. Vergnes, B., Della Valle, G. and Tayeb, J. (1993). A Specific Slit Die Rheometer for Extruded Starchy Products. Design, Validation and Application to Maize Starch, *Rheologica Acta*, **32**: 465–476.

11. Della Valle, G., Colonna, P. and Patria, A. (1996). Influence of Amylose Content on the Viscous Behavior of Low Hydrated Molten Starches, *Journal of Rheology*, **40**(3): 347–362.

12. Della Valle, G., Boché, Y., Colonna, P. and Vergnes, B. (1995). The Extrusion Behavior of Potato Starch, *Carbohydrate Polymer*, **28**: 255–264.

13. Martin, O., Avérous, L. and Della Valle, G. (2003). In-line Determination of Plasticized Wheat Starch Viscoelastic Behavior: Impact of Processing, *Carbohydrate Polymers*, **53**: 169–182.

14. Willett, J.L., Jasberg, B.K. and Swanson, C.I. (1995). Rheology of Thermoplastic Starch: Effect of Temperature, Moisture Content, and Additives on Melt Viscosity, *Polymer Engineering and Science*, **35**(2): 202–210.

15. Aichholzer, W. and Fritz, H.G. (1998). Rheological Characterization of Thermoplastic Starch Materials, *Starch*, **50**(2,3): 77–83.

16. Avérous, L., Fauconnier, N., Moro, L. and Fringant C. (2000). Blends of Thermoplastic Starch and Polyesteramide: Processing and Properties, *Journal of Applied Polymer Science*, **76**: 1117–1128.

17. Martin, O. and Avérous, L. (2001). Poly (lactic acid): Plasticization and Properties of Biodegradable Multiphase Systems, *Polymer*, **42**: 6209–6219.

18. Huneault, M.A. and Li, H. (2007). Morphology and Properties of Compatibilized Polylactide/Thermoplastic Starch Blends, *Polymer*, **48**: 270–280.

19. Matzinos, P., Tserki, V., Kontoyiannis, A. and Panayiotou, C. (2002). Processing and Characterization of Starch/Polycaprolactone Products, *Polymer Degradation and Stability*, **77**: 17–24.

20. Avérous, L., Moro, L., Dole, P. and Fringant, C. (2000). Properties of Thermoplastic Blends: Starch-Polycaprolactone, *Polymer*, 41: 4157–4167.

21. Li, G., Sarazin, P., Yuan, Z. and Favis, B.D. (2005). *Annual Technical Conference - Society of Plastics Engineers*, 63rd: 2092–2096.

22. Schwach, E. and Averous, L. (2004). Starch-based Biodegradable Blends: Morphology and Interface Properties, *Polymer International*, **53**: 2115–2124.

23. Tatarka, P.D. and Cunningham, R.L. (1998). Properties of Protective Loose-Fill Foams, *Journal of Applied Polymer Science*, **67**: 1157–1176.

24. Tatarka, P.D. (1996). Electrical Resistance Characteristics of Starch Foams, *Journal of Environmental Polymer Degradation*, **4**(3): 149–156.

25. Willett, J.L. and Shogren, R.L. (2002). Processing and Properties of Extruded Starch/Polymer Foams, *Polymer*, **43**: 5935–5947.

26. Bhatnagar, S. and Hanna, M.A. (1995). Physical, Mechanical, and Thermal Properties of Starch-based Plastic Foams, *Transaction of ASAE*, **38**(2): 567–571.

27. Sato, Y., Iketani, T., Takishima, S. and Masuoka, H. (2000). Solubility of Hydrofluorocarbone (HFC-134a, HFC-152A) and Hydrochloro-fluorocarbon

(HCFC-142B) Blowing Agents in Polystyrene, *Polymer Engineering and Science*, **40**(6): 1369–1375.

28. Daigneault, L.E., Handa, Y.P., Wong, B. and Caron, L.M. (1998). Solubility of Blowing Agents HCFC 142b, HFC 134a, HFC 125 and Isopropanol in Polystyrene, *Journal of Cellular Plastics*, **34**: 219–230.

29. Gendron, R., Vachon, C., Champagne, M.F. and Delaviz, Y. (2004). Foam Extrusion of PS Blown with a Mixture of HFC-134a and Isopropanol, *Cellular Polymers*, **23**(1): 1–24.